

A comprehensive flight plan risk assessment and optimization method considering air and ground risk of UAM

Yu Su, Yan Xu, Gokhan Inalhan
School of Aerospace, Transport and Manufacturing
Cranfield University
Bedford, United Kingdom
(yu.su, yanxu, inalhan)@cranfield.ac.uk

Abstract—Inspired by risk analysis assistance service and flight plan preparation / optimization service in U-space service, this paper investigates a flight plan risk assessment and optimization method for future urban air mobility. The quantitative risk assessment of the flight plan is divided into two parts: the ground and air risks of the flight plan. After evaluating the risk of the flight plan, optimization suggestions are given to guide the path planning algorithm to optimize the flight plan at low risk. The quantitative risk assessment of the flight plan corresponds to risk analysis assistance service in U-space service, and the procedure to give optimization suggestions correspond to flight plan preparation / optimization service in U-space service. This paper selects the task scenario of logistics drone cargo transportation and carries out risk assessment on the specific flight plan. From the assessment results, when the flight plan crosses the pedestrian intensive area on the ground or the road with high-speed vehicles, the risk value of the corresponding flight plan segment increases significantly. When the flight plan segment approaches the area near the airport or intersects with other UAM participants with the same mission time window, the corresponding risk value is also high. After obtaining the risk assessment results, the targeted optimization suggestions are given to guide the path planning algorithm to optimize the flight plan at low risk. The risk of the optimized flight plan has been significantly reduced.

Index Terms—urban air mobility, flight plan, risk assessment

I. INTRODUCTION

A. Research background

In the urban aerial environment, unmanned aircraft system (UAS) and small manned aircraft are already being applied for various purposes such as traffic monitoring [1] nowadays. Also, they are plans for smart cities in the near future [2], [3] and a core component of Urban Air Mobility (UAM) [4].

UAM enables cooperative, highly automated, cargo delivery or passenger air transportation services in and around urban areas. In the popularization of UAM, integrating UAM into urban and suburban airspace is challenging, as it entails risks from a safety perspective.

Therefore, it is very necessary to conduct a risk assessment for the flight plan of UAM, assess the risk distribution of the existing flight plans to mission airspace, analyze whether there

are parts of the flight plan that pose risks to ground property and air vehicles, and propose revisions in a targeted manner.

B. Previous work

The European Union has developed a vision called U-Space to facilitate the phased introduction of procedures and a set of services for safe, efficient and secure access to airspace for large numbers of drones. In the blueprint of U-space services, risk analysis assistance and flight plan preparation / optimization are both identified as extended U2 services in CORUS.

The service called risk analysis assistance will perform risk assessment to the preliminary flight plan [5]. For risk assessment, Joint Authorities for Rulemaking on Unmanned Systems (JARUS) has developed the Specific Operational Risk Assessment (SORA). It is a novel approach which can evaluate the risk level of an UAS operation plan [6]. In addition to SORA, Ref [7] proposed risk assessment models of UAS over road networks. Going further, they investigate the feasibility of a long-range inspection mission of railways by UAS [8].

The service called flight plan preparation / optimization can be divided into two parts, one is to perform risk assessment before generating the flight plan and then generate a low-risk flight plan according to the evaluation results [9], and the other is to optimize the existing flight plan with low risk [10]. For the preparation of the flight plan, SORA focuses on assigning to an UAS operation two classes of risk, a ground risk class (GRC) and an air risk class (ARC). The SORA allows operators to utilise certain or mitigating measures to reduce both risk-classes [11], [12]. Ref [13]–[15] proposed the concept of risk cost map that associates discretized locations of the space with a suitable risk cost and guided flight plan generation with the risk cost map. For the optimization of the flight plan, [16], [17] integrates the flight plan with multiple airspace, and optimize the flight plan to reduce fuel consumption.

C. Research gap and contribution of this paper

For the risk assessment of flight plans, many risk assessment models are currently targeted at specific objects. For example,

Refs [7] and [8] put forward the risk assessment of the ground roads for the flight plan; Refs [18], [19], [20] and [21] focus on the risks of ground areas or buildings; Ref [22] focuses on risks in airspace. However, in the actual UAM operation process, there will be both air and ground risks, which requires a risk assessment model to comprehensively assess mission risks. SORA process is also far from being finished. The GRC/ARC lookup table is based on a simple scoring. Finally, after the risk assessment of the flight plan, how to optimize it is a problem to be solved.

The main contribution of this paper is that it makes up the gap in the research field of UAM flight plan comprehensive risk assessment, quantitatively analyzes the flight plan risk and gives targeted optimization advisories.

II. RESEARCH MOTIVATION AND STRUCTURE

As mentioned above, risk analysis assistance service and flight plan preparation / optimization service are two important components of U-Space services, which ensure the safety of aircraft flight plan.

Inspired by the above two important services, the research motivation of this paper is to combine the them to achieve flight plan risk assessment and optimization. Firstly, a comprehensive flight plan risk assessment of urban air traffic participants to air and ground property is carried out, and then if needed (based on the assessment results), the corresponding optimizations are proposed for the purpose of ensuring the flight plan associated risk under a certain level.

The flow chart of the proposed flight plan risk assessment and optimization method is shown in Figure 1. As shown in the flow chart, firstly, the flight plan data uploaded by the flight plan generator or the risk assessment system user (e.g., operator) is received in a unified format, the aircraft performance information and weather forecast information at the time of the mission are also received, which will be combined with external environmental information for risk assessment. The risk assessment is divided into two parts, the flight plan's risk to the ground and air.

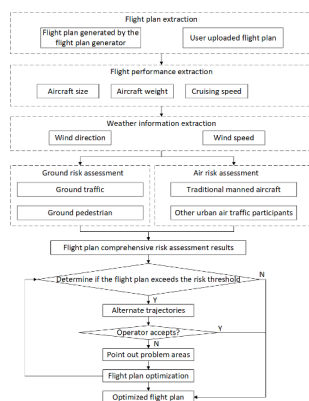


Fig. 1. Flow chart of the flight plan risk assessment and optimization method.

For the risk assessment to the ground, this paper will focus on the following two parts: risk assessment on roads and

pedestrians. As for flight risks in the air, this paper will focus on the traditional aircraft cruising at high altitude and urban air traffic participants cruising at low altitude.

The obtained maximum risk value of the flight mission will be compared with the risk threshold. If it is greater than the risk threshold, a few alternative trajectories will be proposed for the operators to select. If the operator does not accept any alternative trajectories, the problematic risky areas traversed by the preliminary trajectory will be pointed out so that operators can plan new ones on their own to mitigate the risk. The new flight plan generated by the operator will be returned to reassess whether it exceeds the risk threshold.

III. FLIGHT PLAN RISK ASSESSMENT AND OPTIMIZATION

The goal of this section is to propose a framework for comprehensive risk assessment and corresponding optimization of flight plan, so as to combine risk analysis assistance and flight plan preparation / optimization services in U-Space services and realize flight plan management considering risk.

A. Flight plan extraction

As shown in Figure 1, the flight plan risk assessment and optimization system will first extract the existing flight plan. These flight plans are defined as unified standards for subsequent risk calculation and optimization opinions. The schematic diagram of flight plan is shown in Figure 2. In the figure, the green mark represents the starting point of the flight plan, the red mark represents the end point of the flight plan, the yellow marks represent the waypoints constituting the flight plan, and the blue line segments represent the flight route between waypoints which are simplified as a straight line segment connecting two points.

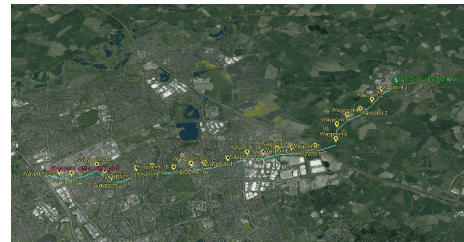


Fig. 2. Schematic diagram of flight plan.

In the above flight plan, the starting and end point of the flight plan contains the information of take-off/landing time, take-off / landing point longitude, latitude and altitude; the waypoints in the flight plan contain the information of longitude, latitude and altitude information; the flight paths connecting waypoints (straight line segments) contain the information of cruise speed, heading angle and pitch angle.

B. Weather information extraction

Weather conditions are an essential consideration in the risk assessment of aircraft. The effect of wind will affect the flight trajectory or impact speed of the aircraft after failure. In practice, scholars mainly consider the impact of wind on

flight risk in two ways: weather forecast or real-time wind information.

According to ref [23], the wind direction and wind force are obtained through weather forecast before flight. However, during the actual flight mission, the wind situation may be different from the weather forecast. In that situation, the authors used a stochastic manner deal with the uncertainty during the evaluation of the ground location affected by the fall impact. They chose a two-dimensional parameterization of the wind and the associated assumptions of the probability distribution, normal distribution for wind magnitude and uniform distribution for wind heading angle.

Another method is to have real-time information of wind conditions during the flight. In [24], wind information achieved by using airborne sensor along with estimation algorithms, therefore no statistical assumption will be taken.

In this paper, we combine the above two methods with risk analysis assistance and flight plan preparation / optimization services, then it is integrated into the risk assessment and optimization framework proposed in this paper. In the risk assessment and targeted optimization of flight plan before mission flight, we use the wind data from weather forecast. During the mission flight, the real-time wind direction and wind data will also be collected by the aircraft's airborne sensors. The flight plan optimization service will use the data to re evaluate the flight plan and correct the optimization scheme in time.

The resistance F_{wind} received by the aircraft in the wind is shown in the following equation. In order to simplify the evaluation process, it is assumed that the windward area of the aircraft in all directions of the horizontal plane is approximately equal, which is $A_{horizontal}$. Where v_{wind} represents wind speed.

$$F_{wind} = \frac{\rho v_{wind}^2 C_D A_{horizontal}}{2} \quad (1)$$

C. Risk assessment

1) *Definition and evaluation of risk:* According to ref [25], there might be three processes a crash incident will cause fatality: failure of UAM; the failed UAM hitting other property; and causing fatality damage after impact. Based on these three processes, the risk cost of UAM is defined as the number of fatalities per hour in this paper. The risk cost is calculated as Eq. (2).

$$R = P_{crash} \cdot P_{impact} \cdot P_{fatality} \quad (2)$$

Where R is the risk cost, P_{crash} is the probability of UAM failure, P_{impact} is the probability to impact an object, and $P_{fatality}$ is the fatality rate, which is mainly associated to the function of kinetic energy.

For the probability of an aircraft crash P_{crash} , in the urban low-altitude mission environment, there are many types of aircraft involved in traffic. This complicates the identification of crash probabilities. The main UAM participants may include conventional manned aircraft (such as helicopter),

high performance vehicle (HPV), such as urban air taxis, and standard performance vehicle (SPV), such as delivery drone and aerial photography drone. Therefore, traditional aviation risk assessment standards cannot be used to estimate the probability of crashes. In this paper, UAM participants are collectively referred to as aircraft, and aircraft is divided into fixed wing aircraft and rotorcraft. The probability of an aircraft crash quantifies the frequency associated with the aircraft accident. Usually, it is consistent with the failure rate of the aircraft system, expressed in flight hours. According to [26], $1/10^5$ flight hours is used as the commercial aviation failure rate, and $1/10^4$ flight hours for HPV. While for SPV, $1/10^3$ flight hours is used.

For the probability to impact an object P_{impact} , considering the risk of aircraft to ground vehicles and pedestrians, P_{impact} is linearly correlated with the number of vehicles or pedestrians affected on the ground after the crash of the aircraft. Considering the risk of aircraft to other air traffic participants located in the airspace, P_{impact} is linearly correlated with the number of collisions per flight hour of the aircraft.

For fatality rate $P_{fatality}$, it is associated with two main factors: impact kinetic energy E_k and shelter factor $c_{shelter}$. The shelter factor is a positive number used to quantify the shelter level of impacted object. This is very important to consider, because the presence of buildings and other obstacles, the vehicle / aircraft itself in the affected area can reduce the kinetic energy at the time of impact, thereby reducing the probability of death. If shelter factors are not evaluated, the resulting risks may be too conservative, especially in urban environments where buildings, vehicles, and trees protect the population. The fatality rate $P_{fatality}$ can be described by Eq. (3). In Eq. (3), α is the impact energy that might cause 50% fatality with $c_{shelter}=0.5$. β is the impact energy threshold required to cause fatality as $c_{shelter}$ approaching zero [27]. In this paper, we set α to 10^6 J and β to 100 J.

$$P_{fatality} = \frac{1}{1 + \sqrt{\frac{\alpha}{\beta} \left(\frac{\beta}{E_k} \right)^{\frac{1}{4c_{shelter}}}}} \quad (3)$$

In order to estimate the impact kinetic energy during aircraft impact, we use the following basic equations:

$$E_k = \frac{mv^2}{2} \quad (4)$$

$$v^2 - v_0^2 = 2ax \quad (5)$$

$$v = v_0 + at \quad (6)$$

$$a = \frac{F}{m} \quad (7)$$

m is aircraft mass, v is the velocity of the aircraft at the time of impact, and a is aircraft acceleration. The gravity on the aircraft can be expressed as:

$$F_{gravity} = mg \quad (8)$$

The resistance of the aircraft is calculated by the following equation, where C_D is the drag coefficient, and A is the windward area of the aircraft:

$$F_{resistance} = \frac{\rho v^2 C_D A}{2} \quad (9)$$

2) *Risk assessment of flight plan to the ground:* After extracting the flight performance information and weather data of the aircraft, the next step is to evaluate the risk of the flight plan to the ground property. In [23], Harbo et al. consider 4 different types of uncontrolled descent of an aircraft: ballistic descent, uncontrolled glide, parachute descent and flyaway. According to the falling characteristics of fixed wing aircraft and rotorcraft, the first two types of descent have been applied in this paper. The latter two models are beyond the scope of this paper.

For the risk assessment of rotorcraft to the ground, we consider the loss of power of rotorcraft during mission flight. For the falling process of the rotorcraft in this situation, it can be regarded as a ballistic descent. Ballistic descent is a situation where the aircraft has lost most of its lift. The aircraft will then enter a (or close to) ballistic descent governed solely by the aerodynamics of the aircraft.

For the risk assessment of fixed wing aircraft to the ground, we consider the case that the aircraft loses power and all control surfaces basically maintain the midpoint position. In this case, the falling process of fixed wing aircraft can be regarded as uncontrolled gliding. The aircraft will enter a descent path governed by the glide ratio.

a) *Analysis of the descent of rotorcraft:* Before the risk assessment of the flight plan to the ground, it is necessary to conduct dynamic modeling of the aircraft and analyze its descent process. This includes the analysis of the falling process of the aircraft, evaluating the horizontal distance of the aircraft from failure to crash, as well as the kinetic energy when it collides with the ground. During the descent of the rotorcraft, the force on it can be expressed by the following equation.

$$\vec{F} = \vec{F}_{gravity} + \vec{F}_{thrust} + \vec{F}_{resistance} \quad (10)$$

According to Eq (9), C_D is the drag coefficient, and A is the projected area above the aircraft. Then the vertical acceleration a_y of aircraft is:

$$a_y = \frac{mg - F_{resistance}}{m} = g - \frac{\rho v_y^2 C_D A}{2m} \quad (11)$$

According to Eq (6), the vertical velocity when hitting the ground v_{yhit} from specified height H is:

$$v_{yhit} = \int_0^t g - \frac{\rho v_y^2 C_D A}{2m} dt = \sqrt{\frac{2mg}{\rho C_D A} \left(1 - e^{-\frac{\rho C_D A H}{m}}\right)} \quad (12)$$

Since the forward wind resistance area of the rotorcraft is small, the horizontal forward resistance is ignored. And the cruising speed of the aircraft is v_{cruise} approximately equal to the horizontal velocity v_{xhit} . The impact kinetic energy E_k of the rotorcraft on the ground is:

$$E_k = \frac{mv_{xhit}^2}{2} + \frac{mv_{yhit}^2}{2} = \frac{mv_{cruise}^2}{2} + \frac{m^2 g}{\rho C_D A} \left(1 - e^{-\frac{\rho C_D A H}{m}}\right) \quad (13)$$

The time it takes for the aircraft to fall from height h to the ground is t_{fall} , The relationship between fall time t_{fall} and flying height h is shown in the following equation:

$$t_{fall} = \sqrt{\frac{2m}{\rho C_D A g}} \cosh^{-1} \left(e^{\frac{\rho C_D A H}{2m}} \right) \quad (14)$$

Then for the rotorcraft, the horizontal threatening distance L_{threat} when the fault occurs is:

$$L_{threat} = v_x \cdot t_{fall} = v_{cruise} \sqrt{\frac{2m}{\rho C_D A g}} \cosh^{-1} \left(e^{\frac{\rho C_D A H}{2m}} \right) \quad (15)$$

Finally, we consider the impact of wind during falling. The deviation distance $W_{distance}$ of the rotorcraft falling area caused by the wind can be expressed by the following equation, and the deflection direction is opposite to the real-time wind direction.

$$W_{distance} = \frac{a_x t_{fall}^2}{2} = \frac{v_{wind}^2 A_{horizontal}}{2Ag} \cdot \left[\cosh^{-1} \left(e^{\frac{\rho C_D A H}{2m}} \right) \right]^2 \quad (16)$$

b) *Analysis of the descent of fixed wing aircraft:* During the descent of the fixed wing aircraft, the force on it can be expressed by the following equation.

$$\vec{F} = \vec{F}_{lift} + \vec{F}_{gravity} + \vec{F}_{thrust} + \vec{F}_{resistance} \quad (17)$$

The lift of aircraft can be expressed as the following equation, where C_y is the lift coefficient, ρ is the air density, S is the wing area.

$$F_{lift} = \frac{C_y \rho v^2 S}{2} \quad (18)$$

As mentioned above, the descent of fixed wing aircraft can be regarded as a glider, and the lift-to-drag ratio is equal to the glide ratio. In the following equation, S_{lift} is the lift-to-drag ratio, K is the glide ratio, L_{threat} is the dangerous range of fixed wing aircraft failure, and H is the flight altitude.

$$S_{lift} = K = \frac{F_{lift}}{F_{resistance}} = \frac{L_{threat}}{H} \quad (19)$$

Fixed wing aircraft failure hazard range L_{threat} can be expressed as:

$$L_{threat} = HK = \frac{HF_{lift}}{F_{resistance}} \quad (20)$$

$$L_{threat} = H \cdot \frac{C_y \rho v^2 S}{2} \cdot \frac{2}{\rho v^2 C_{DA}} = \frac{H C_y S}{C_{DA}} \quad (21)$$

According to [23], ignoring the complex force and speed changes when gliding without power, and simplifying the process to a uniform falling motion, the horizontal speed is defined as the gliding speed v_{glide} and remains unchanged. The relationship between the horizontal velocity v_{xhit} and the vertical velocity v_{yhit} at the time of impact is:

$$\frac{v_{yhit}}{v_{xhit}} = \frac{H}{L_{threat}} = \frac{C_{DA}}{C_y S} \quad (22)$$

The impact kinetic energy E_k of fixed wing aircraft on the ground is:

$$E_k = \frac{m v_{glide}^2}{2} \cdot \left[1 + \left(\frac{C_{DA}}{C_y S} \right)^2 \right] \quad (23)$$

The fixed wing aircraft descent time t_{fall} can be calculated by the following equation:

$$t_{fall} = \frac{L_{threat}}{v_{glide}} = \frac{H C_y S}{C_{DA} v_{glide}} \quad (24)$$

Finally, we consider the impact of wind during falling. The deviation distance $W_{distance}$ of the fixed wing aircraft falling area caused by the wind can be expressed by the following equation, and the deflection direction is opposite to the real-time wind direction.

$$W_{distance} = \frac{a_x t_{fall}^2}{2} = \frac{\rho v_{wind}^2 A_{horizontal} H^2 C_y^2 S^2}{4m C_{DA}^2 v_{glide}^2} \quad (25)$$

c) *Definition of ground risk area of flight plan:* According to the definition of flight plan, flight plan is composed of waypoints and straight-line segments connected between waypoints. The risk assessment of flight plan can be defined as the assessment of route segments between each waypoint. Before conducting risk assessment, it is necessary to determine the specific areas where the flight plan may affect the ground.

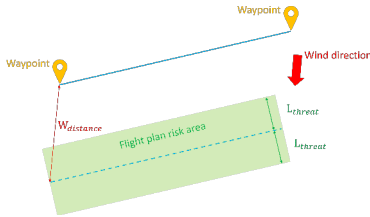


Fig. 3. Impact area of flight plan on the ground.

Figure 3 is a top view of the impact area of the flight plan on the ground. The yellow mark in the figure represents two waypoints in the flight plan, and the blue line segment is the route connecting the two waypoints. The direction of the red arrow is the current wind direction, and the green area is the area on the ground that may be affected by the flight plan.

The horizontal offset of the affected area from the flight plan is deviation distance $W_{distance}$ mentioned above. The length of the affected rectangular area is the length of the straight line segment connecting the two waypoints, and the width is $2L_{threat}$.

d) *Ground risk assessment of flight plan:* After evaluating the risk area distribution of the flight plan on the ground, we take the straight-line segment connecting waypoints as the evaluation unit to evaluate the ground risk of the whole flight plan. The risks on the ground are divided into two categories: ground vehicles and pedestrians. In order to more accurately assess the risk of UAM to pedestrians on the ground, we have divided the ground areas of the city according to their functions. Multidimensional Open Data of Urban Morphology (MODUM) method is used to classify the study area. The aircraft mission area is divided into the following types according to different functions: Suburban Landscapes, Railway Buzz, The Old Town, Victorian Terraces, Waterside Settings, Countryside Sceneries, High Street and Promenades and Central Business District.

As mentioned above, risk is defined by Eq. (2). It consists of failure probability P_{crash} , impact probability P_{impact} , and fatality rate $P_{fatality}$. Failure probability P_{crash} is expressed in flight hours and be set to $1/10^5$ for the commercial aviation, $1/10^4$ for HPV, and $1/10^3$ for SPV.

Impact probability P_{impact} is linearly correlated with the number of vehicles or pedestrians affected by the crash of the aircraft. In order to estimate the number of affected ground vehicles and pedestrians, it is necessary to estimate the density of vehicles / pedestrians in the falling area and the size of the area affected by the aircraft falling on the ground.

For the density of road vehicles, the real-time traffic information of the road can be obtained through the existing guidance software, such as Google maps. As described in [28] and [29], government population data is aggregated for the protection of privacy. In order to obtain more accurate population distribution data, dasymetric mapping was proposed [30], [31]. This method uses auxiliary data to improve the resolution of population density distribution. Based on this method, the multi-class dasymetric mapping method is developed. The area is partitioned into several residential classes (e.g., low density, medium density, high density) associated with different population densities [32]. Inspired by multi-class dasymetric mapping method, combined with the above-mentioned MODUM region division method and considered the difference of population density in different functional areas [33], we propose a method to evaluate the distribution of population density by using functional areas as auxiliary data.

As shown in Table I, based on the regional average population density data given by the government, we give the population density weight to each different functional part of the region. Refer to [32] for specific weight value. After obtaining the average population density of the study area and the population distribution weight of each part in the area, the population density ρ_{people} of each part can be obtained.

TABLE I
THE DISTRIBUTION OF POPULATION DENSITY WEIGHTS

| Area type | weight |
|----------------------------|--------|
| None | 0 |
| High Street and Promenades | 0.05 |
| Railway Buzz | 0.05 |
| Waterside Settings | 0.05 |
| Countryside Sceneries | 0.075 |
| Suburban Landscapes | 0.075 |
| The Old Town | 0.2 |
| Victorian Terraces | 0.2 |
| Central Business District | 0.3 |

For the size of the affected area, Figure 4 and Figure 5 shows the risk areas of the flight plan on the ground roads and functional areas respectively. The affected area is the risk area of the flight plan on the ground and the overlapping part of the road area / functional area divided based on MODUM.

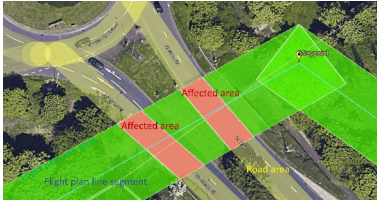


Fig. 4. Schematic diagram of affected areas of roads.



Fig. 5. Schematic diagram of the affected area of divided area.

The final impact probability P_{impact} is shown in Eq. (26). It is a linear function to the number of affected cars or pedestrians. In the equation, C_{linear} is linear coefficient, $\rho_{car/people}$ is the density of vehicles or pedestrians in the affected area, and $A_{affected}$ is the the size of the affected area.

$$P_{impact} = C_{linear} \cdot \rho_{car/people} \cdot A_{affected} \quad (26)$$

The fatality rate $P_{fatality}$ is related to two main factors: shelter factor $c_{shelter}$ and impact kinetic energy E_k . The shelter factor defines the shelter level when the aircraft collides with ground property. Referring to [27], the fatality rate $P_{fatality}$ in this paper is described by Eq. (3) where α is the impact energy that might cause 50% fatality with $c_{shelter}=0.50$, which is set to 10^6 J. β is the impact energy threshold required to cause fatality as $c_{shelter}$ approaching zero, which is set to 100 J.

When estimating the impact of an aircraft fall on pedestrians on the ground, it is necessary to consider the sheltering effect

of buildings and trees on the impact. The shelter factor defines the shelter level of the map. The shelter factor is a positive number used to quantify the shelter level of people in the area. The value of the shelter factor $c_{shelter}$ is shown in the Table II which varies with zone type.

TABLE II
THE VALUE OF THE SHELTER FACTOR $c_{shelter}$

| Shelter type | $c_{shelter}$ |
|----------------------------|---------------|
| None | 1 |
| High Street and Promenades | 0.8 |
| Railway Buzz | 0.75 |
| Waterside Settings | 0.7 |
| Ground vehicles | 0.5 |
| Countryside Sceneries | 0.5 |
| Suburban Landscapes | 0.45 |
| The Old Town | 0.35 |
| Victorian Terraces | 0.3 |
| Central Business District | 0.25 |

After determining the shelter factor, next step is to estimate the impact kinetic energy during aircraft collision. As mentioned above, the value of the absolute velocity \vec{v}_{xhit} of rotorcraft hitting the ground is v_{cruise} , of fixed wing aircraft hitting the ground is v_{glide} , and the direction is the heading of the flight plan segment. The velocity of the aircraft impacting the ground can be expressed by Eq. (27) and the impact kinetic energy of aircraft on ground vehicles or pedestrians is shown in Eq. (28). In the following equations, \vec{v}_{hit} is the velocity vector of the aircraft impacting the ground vehicle or pedestrian. \vec{v}_{car} is the vehicle speed vector on the ground road. The direction of the vector is the traffic flow direction of the ground road, and the value of the vector is the speed limit of the ground road.

$$\vec{v}_{hit} = \begin{cases} \vec{v}_{xhit} - \vec{v}_{car} + \vec{v}_{yhit} & (car) \\ \vec{v}_{xhit} + \vec{v}_{yhit} & (pedestrian) \end{cases} \quad (27)$$

$$E_k = \frac{m |\vec{v}_{hit}|^2}{2} \quad (28)$$

According to the shelter factor $c_{shelter}$ and impact kinetic energy E_k , the fatality rate $P_{fatality}$ can be obtained by Eq. (3). Now we have failure probability P_{crash} , impact probability P_{impact} , and fatality rate $P_{fatality}$, Eq. (2) can be used to calculate the risk value of the flight plan to the ground.

3) *Risk assessment of flight plan to the air:* When the UAM participants operate together in urban airspace, the risk assessment between them is very important.

In this paper, we divide UAM participants into two parts, traditional manned aircraft operating at high altitude and urban air traffic vehicles operating at low altitude, such as logistics UAS or air taxis. Because the air traffic management system of traditional manned aircraft has been fully developed, the risk assessment between traditional manned aircraft is not the focus of this paper. In this paper, our research focuses on the risks of the flight plan of low altitude urban air traffic aircraft

to the traditional high altitude manned aircraft and risks to other low-altitude air traffic participants in the event of an emergency.

a) Risk of flight plan to traditional manned aircraft:

The risk issues of the flight plan of low altitude urban air traffic aircraft and traditional manned aircraft operating at high altitude are crucial to the UTM-ATM integration [34]. For civil manned aircraft, the cruising altitude is usually 6000 to 12600 meters. However, the operating altitude of ordinary urban air traffic aircraft is far lower than this altitude. Therefore, we only consider the risks to the flight plan during the takeoff and landing phase of a traditional manned aircraft. For aircraft air risk assessment, we continue to use the definition of risk in Eq. (2). Failure probability P_{crash} between manned aircraft and unmanned aircraft is set to $1/10^3$ flight hours.

Referring to [25], impact probability P_{impact} is linearly correlated with the number of collisions $N_{aircraft}$ between manned aircraft and unmanned aircraft per flight hour. It can be calculated by Eq. (29).

$$P_{impact} = C_{linear} \cdot N_{aircraft} \quad (29)$$

To ensure public airspace safety, DJI sets GEO Zones around airports to regulate UAV flights. Referring to the zone division by DJI, the airspace division of the airport area in this paper is shown in the 6.

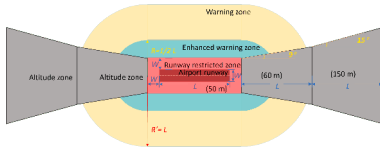


Fig. 6. Schematic diagram of the airspace division.

As shown in the above figure, the airspace near the airport is divided into the following parts: Runway restricted zone, Altitude zone, Enhanced warning zone, Warning zone. The Runway restricted zone covers airport runways in a cube shape which height is 50m. The Altitude Zone is an area of restricted flight altitude. Each of these zones consists of two parts. Part one is a 60-meter height-restricted area, which length is equal to the length of the runway. It extends outward from the four corners of a Runway restricted zone at an angle of 9° . Part two is a 150-meter height-restricted area, which length is equal to the length of the runway, and from the corners of part one at an angle of 15° . An Enhanced warning zone is a circular area that extends outwards from the Runway restricted zone and a Warning zone is an extension of the Enhanced warning zone.

The number of collisions $N_{aircraft}$ between manned aircraft and unmanned aircraft per flight hour can be calculated by Eq. (30). In the air risk assessment of a flight plan, the risk area of the flight plan can be defined as a rectangular area with the flight plan line segment as the axisymmetric center, the length as the length of the flight plan line segment, and the width as the maximum width of the aircraft. In the equation, $\rho_{aircraft}$ represents the density of manned aircraft at the overlap of

the vertical projection of the risk area on the ground and the projection of the airport area on the ground. $A_{affected}$ represents the overlapping area of the vertical projection of the flight plan risk area and the airport area on the ground.

$$N_{aircraft} = \rho_{aircraft} \cdot A_{affected} \quad (30)$$

It should be noted that the height range of areas Warning zone and Enhanced warning zone is 150m, that of area Runway restricted zone is 50m, that of area close to area Runway restricted zone is 60m, and that of outside Altitude Zone is 150m. Only when the average altitude of the flight plan segment is within the altitude range of the above airport areas, the intersection of the flight plan risk area and the airport area will be considered.

Finally, it is necessary to evaluate the air impact kinetic energy and estimate fatality rate $P_{fatality}$. Eq. (31) is the assessment of kinetic energy for air impact. v_{cruise} refers to the cruise speed of aircraft flying according to the flight plan, and v_{air} refers to the takeoff/landing speed of manned aircraft at the airport. Fatality rate $P_{fatality}$ can be calculated by Eq. (3) where the shelter factor is set as 0.5. Eq. (2) can be used to calculate the risk value of the flight plan to traditional manned aircraft.

$$E_k = \frac{m(v_{cruise} + v_{air})^2}{2} \quad (31)$$

b) Flight plan risks to other urban air traffic participants experiencing emergencies: The Federal Aviation Administration (FAA) maintains the safety and efficiency of National Airspace System. As with cars on the road, there are rules that cover aircraft in the sky to ensure safety. In special circumstances, the FAA may temporarily restrict access to certain designated areas of our airspace, much in the same way a city or state may block off access to a street when necessary. These airspace restrictions are called Temporary Flight Restriction (TFR).

Referring to the above concept, when other UAM participants encounter an emergency situation during mission execution, the U-space service provider (USSP) responsible for the airspace will delineate TFR areas in the vicinity of UAM participants experiencing emergencies. Considering that the aircraft cannot continue to fly according to the original plan after an emergency, and the flight direction is uncertain, the vertical projection on the ground of the aircraft location at the time of failure is taken as the center of the circle, and the possible threat distance is taken as the radius, and a geographical fence extending upward to an infinite height is set, i.e., a temporary flight restricted area.

NASA has developed a detect and avoid (DAA) concept for UAS to avoid collision risk during simultaneous operation [35]. DAA concept includes a mathematical definition of well clear to characterize a well-clear boundary and a suite of algorithms that provide situational awareness of this well-clear boundary to UAS operators [36].

Inspired by the well-clear boundary concept, this paper relates the flight plan risk to other urban air traffic participants

experiencing emergencies to the overlapping area of the TFR and the flight plan risk area.

In this case, failure probability P_{crash} is set to $1/10^3$ flight hours, impact probability P_{impact} can be calculated by Eq. (32), where $S_{overlapping}$ is the overlapping area of the projection on the ground of the temporary flight restriction area and the flight plan risk area.

The velocity for calculating the impact kinetic energy E_k can be calculated by the cruise speed v_{cruise} of the vehicle executing the flight plan, and $P_{fatality}$ can be calculated by Eq. (3) where the shelter factor is set as 0.5. Eq. (2) can be used to calculate the risk value of the flight plan to other urban air traffic participants.

$$P_{impact} = C_{linear} \cdot S_{overlapping} \quad (32)$$

D. Flight plan low risk optimization

Based on the original flight plan, some modifications to the original flight plan should be made according to the identified high-risk locations. The optimization principle of flight plan is shown in Figure 7.

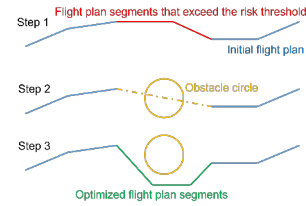


Fig. 7. Flight plan optimization principle.

In the above figure, the blue line segment represents the initial flight plan, the red line segment represents the line segment that exceeds the risk threshold, the yellow dotted line represents the auxiliary line for finding the centre of the obstacle circle. The yellow circle represents the obstacle circle, the diameter is determined by the risk value. The green line segment is the new path after re-passing the path planning. The flight plan optimization process is as follows: step 1 is the risk assessment on the existing flight plan (straight lines between waypoints). In the step 2, the superimposed weight of the risk value is used as the diameter of the obstacle circle, and the centre of the circle is the midpoint of the high-risk line segment, or the midpoint of the line connecting the endpoints of several consecutive high-risk line segments. In the step 3, the route segment exceeding the risk threshold is deleted, and the obstacle circle is added to the map. This information is combined with the path planning algorithm to generate a new route segment between the breakpoints of the deleted route segment, and return to step 1 for risk reassessment. If there is any part exceeding the risk threshold, continue to stack the corresponding obstacle circle.

IV. CASE STUDY

In this section, we simulate a mission scenario where a courier multi-rotor drone takes off from Cranfield University

Airport to deliver packages to the VTOL airport at the train station in the city centre of Milton Keynes. The study areas selected as the town Milton Keynes near Cranfield University. The aircraft type is selected as rotorcraft for package delivery. The aircraft type is selected as rotorcraft for package delivery. The specific parameters of the aircraft are shown in table III.

TABLE III
AIRCRAFT PERFORMANCE PARAMETERS

| | |
|---|---------------------|
| Aircraft mass m | 1.4 kg |
| Cruising speed v_{cruise} | 6.5 m/s |
| Cruising altitude H | 50 m |
| Vertical windward area A | 0.02 m ² |
| Horizontal windward area $A_{horizontal}$ | 0.15 m ² |
| Drag coefficient C_D | 0.45 |

Through the above evaluation model, the risk of the example flight plan is evaluated. The following pictures show the risk assessment of the flight plan on different objects. The color of the flight plan segment represents the risk value of the segment. The rainbow bar in the pictures represent the risk value of the flight plan line segment. The risk value changes from high to low from red to green. The risk assessment of flight plan to ground traffic is shown in Figure 8. It can be seen from the figure that when the route crosses the road and the road vehicles travel at a high speed, the route segment risk value of the flight plan is high.

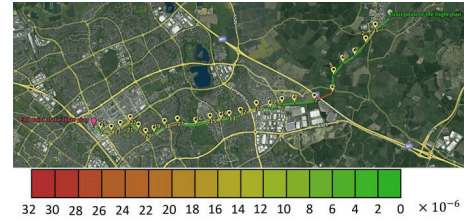


Fig. 8. Risk of flight plan to the ground traffic.

The risk assessment of the flight plan to ground pedestrians is shown in Figure 9, and the ground area is divided by using the method of MODUM. When the flight plan crosses different population density areas, the larger the overlap area between the risk area of the flight plan on the ground and the ground functional area, the higher the population density of the ground functional area, the higher the risk value of the flight plan segment.

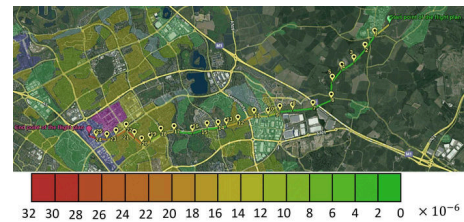


Fig. 9. Risk of flight plan to the ground pedestrians.

The risk assessment of the flight plan to the ground is shown in Figure 10. As shown in the figure, the closer to the densely populated area in the city center, or the flight plan segment across the expressway, the higher the corresponding risk value.

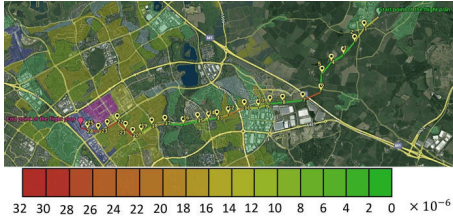


Fig. 10. Risk of flight plan to the ground.

The risk assessment of flight plan on other UAM participants in the airspace is shown in Figure 11. The upper right corner of the figure shows the airspace division of Cranfield airport. The red area is runway restricted zone, the blue area is enhanced warning zone, the yellow area is warning zone, the blue and gray areas are altitude zone.

The red UAM in Figure 11 has suffered an emergency. For the safety of other traffic participants in the airspace, based on the zoning method described above, a circular TFR region is generated considering the uncertainty of the flight direction in case of an aircraft emergency, as shown in the red circular area in the figure.

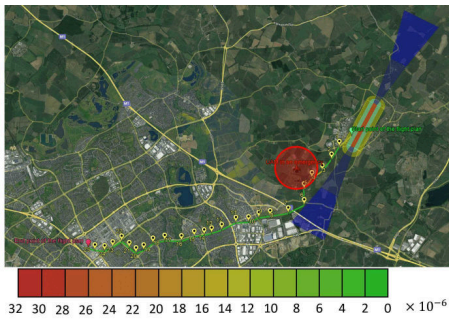


Fig. 11. Risk of flight plan to the air.

Combined with the results of the above risk assessment, the comprehensive risk assessment of the flight plan is shown in Figure 12.

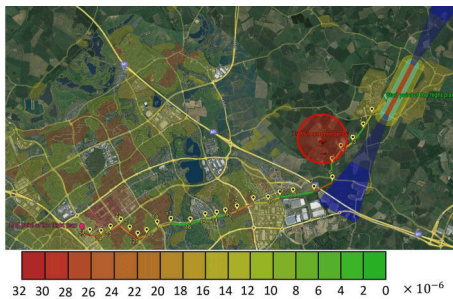


Fig. 12. Comprehensive risk assessment of the flight plan.

After obtaining the risk assessment results of the flight plan, carry out low-risk optimization of the flight plan. As shown in the Figure 13, the flight plan segments near the end of the flight plan exceeds the risk threshold. The yellow circle is the obstacle circle, which takes the midpoint of the yellow dotted line connecting the end point and the waypoint 20 as the center of the circle, and the radius is obtained by superimposing the weight of the risk value. After the obstacle circle is obtained, the path planning algorithm is used to re route in the problem area, and the optimized route segments are shown in the green line in the figure.

As can be seen from Figure 13, the obstacle circle covers the most densely populated functional area in the city center (purple functional area in Figure 12). Through the path planning algorithm, the new green leg bypasses the high-risk area. After low-risk cycle optimization, the risk values of all segments on the flight segment are controlled within the threshold, thus ensuring the safety of the mission.

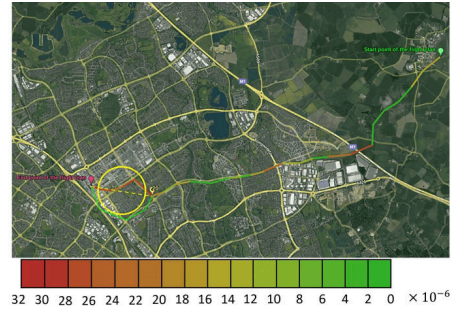


Fig. 13. Flight plan optimization.

V. CONCLUSIONS AND FURTHER RESEARCH

In the field of UAM risk assessment, this paper innovatively proposes a comprehensive risk assessment framework, which quantitatively assesses the ground and air risks of the existing flight plan. We combine risk assessment and flight plan preparation. Quantitative risk assessment result provides a key basis for optimizing the flight plan. After the comprehensive risk assessment of the flight plan, optimization suggestions are put forward according to the assessment results to guide the path planning algorithm to optimize the flight plan at low risk. Through the processing of the risk assessment framework, the possible risk in flight can be mitigated during the pre-flight phase, and thus the operation safety of flight can be improved.

In this study, for the flight plan air risk assessment, the flight plan risk to other UAM participants was considered only in the case of UAM encountering an emergency situation where a TFR was generated. For the case of UAM operating normally in the airspace, collision risk assessment between them is an area that will be addressed in future research.

REFERENCES

- [1] R Reshma, Tirumale Ramesh, and P Sathishkumar. Security situational aware intelligent road traffic monitoring using uavs. In *2016 international conference on VLSI systems, architectures, technology and applications (VLSI-SATA)*, pages 1–6. IEEE, 2016.
- [2] Hamid Menouar, Ismail Guvenc, Kemal Akkaya, A Selcuk Uluagac, Abdullah Kadri, and Adem Tuncer. Uav-enabled intelligent transportation systems for the smart city: Applications and challenges. *IEEE Communications Magazine*, 55(3):22–28, 2017.
- [3] Fei Qi, Xuetian Zhu, Ge Mang, Michel Kadoch, and Wei Li. Uav network and iot in the sky for future smart cities. *IEEE Network*, 33(2):96–101, 2019.
- [4] Parimal Kopardekar. Urban air mobility regional readiness. Technical report, Technical report, 2019.
- [5] Parimal Kopardekar, Joseph Rios, Thomas Prevot, Marcus Johnson, Jaewoo Jung, and John E Robinson. Unmanned aircraft system traffic management (utm) concept of operations. In *16th AIAA Aviation Technology, Integration, and Operations Conference*, pages 1–16. AIAA, 2016.
- [6] Lorenzo Murzilli. Jarus guidelines on specific operations risk assessment (sora), 2017.
- [7] S Bertrand, N Raballand, F Viguier, and F Muller. Ground risk assessment for long-range inspection missions of railways by uavs. In *2017 International Conference on Unmanned Aircraft Systems (ICUAS)*, pages 1343–1351. IEEE, 2017.
- [8] Sylvain Bertrand, Nicolas Raballand, and Flavien Viguier. Evaluating ground risk for road networks induced by uav operations. In *2018 International Conference on Unmanned Aircraft Systems (ICUAS)*, pages 168–176. IEEE, 2018.
- [9] Yu Su and Yan Xu. Risk-based flight planning and management for urban air mobility. In *AIAA AVIATION 2022 Forum*, page 3619, 2022.
- [10] Cristina Barrado, Mario Boyero, Luigi Brucculeri, Giancarlo Ferrara, Andrew Hately, Peter Hullah, David Martin-Marrero, Enric Pastor, Anthony Peter Rushton, and Andreas Volkert. U-space concept of operations: A key enabler for opening airspace to emerging low-altitude operations. *Aerospace*, 7(3):24, 2020.
- [11] Carlos Capitán, Jesús Capitán, Angel R Castano, and Aníbal Ollero. Risk assessment based on sora methodology for a uas media production application. In *2019 International Conference on Unmanned Aircraft Systems (ICUAS)*, pages 451–459. IEEE, 2019.
- [12] L Murzilli et al. Jarus guidelines on specific operations risk assessment (sora), public release edition 2.0, joint authorities for rulemaking of unmanned systems, 2020.
- [13] Stefano Primatesta, Giorgio Guglieri, and Alessandro Rizzo. A risk-aware path planning strategy for uavs in urban environments. *Journal of Intelligent & Robotic Systems*, 95(2):629–643, 2019.
- [14] Stefano Primatesta, Alessandro Rizzo, and Anders la Cour-Harbo. Ground risk map for unmanned aircraft in urban environments. *Journal of Intelligent & Robotic Systems*, 97(3):489–509, 2020.
- [15] Paul P-Y Wu, Duncan Campbell, and Torsten Merz. Multi-objective four-dimensional vehicle motion planning in large dynamic environments. *IEEE Transactions on Systems, Man, and Cybernetics, Part B (Cybernetics)*, 41(3):621–634, 2010.
- [16] Coline Ramee, Kim Junghyun, Marie Deguignet, Cedric Justin, Simon Briceno, and Dimitri N Mavris. Aircraft flight plan optimization with dynamic weather and airspace constraints. 2020.
- [17] Takeshi Tsuchiya, Masahiro Miwa, Shinji Suzuki, Kazuya Masui, and Hiroshi Tomita. Real-time flight trajectory optimization and its verification in flight. *Journal of Aircraft*, 46(4):1468–1471, 2009.
- [18] Jaime Rubio-Hervas, Abhishek Gupta, and Yew-Soon Ong. Data-driven risk assessment and multicriteria optimization of uav operations. *Aerospace Science and Technology*, 77:510–523, 2018.
- [19] Bizhao Pang, Xinting Hu, Wei Dai, and Kin Huat Low. Third party risk modelling and assessment for safe uav path planning in metropolitan environments. *arXiv preprint arXiv:2107.01834*, 2021.
- [20] Qiang Zhou and Mutian Xu. Research on risk assessment of uav to buildings. In *2021 International Conference on Information Control, Electrical Engineering and Rail Transit (ICEERT)*, pages 37–40. IEEE, 2021.
- [21] Uluhan C Kaya, Atilla Dogan, and Manfred Huber. A probabilistic risk assessment framework for the path planning of safe task-aware uas operations. In *AIAA Scitech 2019 Forum*, page 2079, 2019.
- [22] Christopher Lum and Blake Waggoner. A risk based paradigm and model for unmanned aerial systems in the national airspace. In *Infotech@ Aerospace 2011*, page 1424, 2011.
- [23] Anders la Cour-Harbo. Quantifying risk of ground impact fatalities for small unmanned aircraft. *Journal of Intelligent & Robotic Systems*, 93(1):367–384, 2019.
- [24] Michael Bleier, Ferdinand Settele, Markus Krauss, Alexander Knoll, and Klaus Schilling. Risk assessment of flight paths for automatic emergency parachute deployment in uavs. *IFAC-PapersOnLine*, 48(9):180–185, 2015.
- [25] Xinting Hu, Bizhao Pang, Fuqing Dai, and Kin Huat Low. Risk assessment model for uav cost-effective path planning in urban environments. *IEEE Access*, 8:150162–150173, 2020.
- [26] Enrico Petritoli, Fabio Leccese, and Lorenzo Ciani. Reliability and maintenance analysis of unmanned aerial vehicles. *Sensors*, 18(9):3171, 2018.
- [27] Konstantinos Dalamagkidis, Kimon P Valavanis, and Les A Piegł. Evaluating the risk of unmanned aircraft ground impacts. In *2008 16th mediterranean conference on control and automation*, pages 709–716. IEEE, 2008.
- [28] Serkan Ural, Ejaz Hussain, and Jie Shan. Building population mapping with aerial imagery and gis data. *International Journal of Applied Earth Observation and Geoinformation*, 13(6):841–852, 2011.
- [29] Harini Sridharan and Fang Qiu. A spatially disaggregated areal interpolation model using light detection and ranging-derived building volumes. *Geographical Analysis*, 45(3):238–258, 2013.
- [30] Benjamin Semenov-Tian-Shansky. Russia: Territory and population: A perspective on the 1926 census. *Geographical Review*, pages 616–640, 1928.
- [31] John K Wright. A method of mapping densities of population: With cape cod as an example. *Geographical Review*, 26(1):103–110, 1936.
- [32] Cory L Eicher and Cynthia A Brewer. Dasymeric mapping and areal interpolation: Implementation and evaluation. *Cartography and Geographic Information Science*, 28(2):125–138, 2001.
- [33] Jordan Rappaport. Consumption amenities and city population density. *Regional Science and Urban Economics*, 38(6):533–552, 2008.
- [34] SESAR Joint Undertaking et al. European drones outlook study: unlocking the value for europe. 2017.
- [35] Maria C Consiglio, James P Chamberlain, Cesar A Munoz, and Keith D Hoffer. Concepts of integration for uas operations in the nas. Technical report, Technical report, 2012.
- [36] César Munoz, Anthony Narkawicz, James Chamberlain, Maria C Consiglio, and Jason M Upchurch. A family of well-clear boundary models for the integration of uas in the nas. In *14th AIAA Aviation Technology, Integration, and Operations Conference*, page 2412, 2014.

A comprehensive flight plan risk assessment and optimization method considering air and ground risk of UAM

Su, Yu

2022-10-31

Attribution-NonCommercial 4.0 International

Su Y, Xu Y, Inalhan G. (2022) A comprehensive flight plan risk assessment and optimization method considering air and ground risk of UAM. In: 2022 IEEE/AIAA 41st Digital Avionics Systems Conference (DASC), 18-22 September 2022, Portsmouth, Virginia, USA

<https://doi.org/10.1109/DASC55683.2022.9925844>

Downloaded from CERES Research Repository, Cranfield University